ON THE MAGIC CHARACTER OF Al_6Au^-

Michele L. KIMBLE[a], Albert W. CASTLEMAN, Jr.[a1,*], Jose U. REVELES[b] and Shiv N. KHANNA[b1]

[a] *Departments of Chemistry and Physics, The Pennsylvania State University, University Park, PA 16802, U.S.A.; e-mail:* [1] *awc@psu.edu*

[b] *Department of Physics, Virginia Commonwealth University, Richmond, VA 23284, U.S.A.; e-mail:* [1] *snkhanna@vcu.edu*

Received October 30, 2006
Accepted January 30, 2007

In honor and memory of Professor Jaroslav Koutecký, a wonderful person and an excellent scientist, who is dearly missed.

Joint experimental and theoretical studies have been carried out to identify the stability of aluminum gold clusters. The experimental studies where the Al_nAu^- clusters are generated via laser vaporization in a flow reactor and subsequently reacted with oxygen indicate that Al_6Au^- is an exceptionally stable species that is not only resistant to etching by oxygen but also grows in intensity when Al_nAu^- clusters are exposed to oxygen. Theoretical studies indicate that the six aluminum atoms in Al_6Au^- form an octahedron and that the Au atom occupies a hollow site above the triangular face of the octahedron. It is shown that it takes much larger energy to remove an Al or a Au atom compared to that for neighboring sizes, and this accounts for its resistance to oxygen. The special stability is rooted in the electronic spectrum that is marked by a large HOMO-LUMO gap of 1.38 eV, and the system is best described as a nearly free electron gas of 20 electrons.

Keywords: Gold aluminum clusters; Cluster stability; Cluster magic numbers; Laser vaporization; Oxidation; Mass spectrometry; Ab initio calculations.

Gold exhibits a striking progression of behaviors in going from a single atom to the bulk solid. Bulk Au is the most noble metal, resistant to oxidation and corrosion, and has been used for centuries for making utensils, ornaments, and as currency. Unlike the bulk, however, small Au nanoparticles are reactive[1], and small Au_n clusters are known to be potential catalysts for the conversion of CO to CO_2. A single Au atom has a high electron affinity of 2.30 eV that is 0.7 eV smaller than iodine atoms and is indicative of high reactivity. In addition to Au, the other useful metal is aluminum, the third most abundant element in the earth's crust. It has high affinity for oxygen, and bulk Al surfaces in nature are covered with an oxide layer. The reactive

Collect. Czech. Chem. Commun. 2007, Vol. 72, No. 2, pp. 185–196

doi:10.1135/cccc20070185

nature of aluminum continues to smaller sizes, and aluminum nanoparticles and small clusters are generally reactive to oxygen. The only known exception to this oxidation are selected clusters[2–5], for example, Al_{13}^-, Al_{23}^-, Al_{37}^-, ... These sizes, usually called the magic numbers[6,7], owe their unusual resistance to oxygen corrosion, to the finite sizes, and to quantum effects that lead to filled electronic shells in clusters much in the same way as in atoms. Indeed, theoretical studies indicate that the electronic structure of metal clusters can be described within a simple model where the positive ionic core charge is smeared uniformly over a sphere of the size of the cluster. The electronic levels in such a potential well, order as $1s^21p^61d^{10}2s^21f^{14}2p^6$ – compared to $1s^22s^22p^63s^23p^63d^{10}$ – in atoms. Clusters containing 2, 8, 18, 20, 34, 40 electrons then correspond to closed electronic shells and are indeed found to exhibit chemically inert behavior. The chemical stability of the aforesaid aluminum sizes can thus be attributed to the number of valence electrons that result in closed electronic shells. In addition to shell closure, the observed electronic behavior in clusters in which the number of valence electrons deviates from filled shell sizes is found to be reminiscent of open-shell atoms, and this has led to the idea that chosen atomic clusters could be regarded as superatoms[4,8]. Over the past few years, it has been shown that Al_{13}^- mimics an inert gas atom[3], Al_{13} exhibits behaviors reminiscent of a halogen atom[3,9,10], Al_{14} behaves like group II elements[4], and that Al_7^- exhibits multivalent behavior[8]. Identification of these species is currently an important undertaking in cluster science, as it is envisioned that they can form the building blocks of new nanoscale materials.

The purpose of this paper is to present a synergistic effort combining experiments and first principles electronic structure studies to identify an intriguing stable species. Our experiments demonstrate an interesting finding that a combination of two highly reactive species, namely Al_6^- and a single Au atom, leads to an unusually stable species Al_6Au^- that is completely resistant to oxidation. An Al atom has a valence electronic structure of $2s^2 2p^1$, and pure aluminum clusters are known to undergo a transition from a monovalent to a trivalent state[11]. A single Au atom has a valence electronic configuration of $(5d^{10})\ 6s^1$ and contributes a single valence electron. According to the confined electron gas model, outlined above, one could understand this stability with Al_6Au^- having either 8 or 20 valence electrons. Using first-principles electronic structure calculations, we first demonstrate that the Al_6Au^- cluster is stable against the formation of AlO_2, AlO_2^-, Al_2O_2, AuO_2, and AuO_2^- when exposed to O_2, indicative of its observed resistance to etching by oxygen. Further, the cluster is marked by a large HOMO

(highest occupied molecular orbital)-LUMO (lowest unoccupied molecular orbital) gap, attesting to its enhanced stability. Finally, through electronic structure calculations, we propose that the unusual stability is most easily reconciled within a 20-electron model.

METHODS

A fast flow reactor mass spectrometer coupled to a dual rod laser vaporization source, as described in detail previously[12–14], is used to probe the stability of bimetallic aluminum-gold cluster anions. Briefly, the bimetallic clusters are formed in a dual rod laser vaporization source by ablating two metal rods with the second harmonic of a Nd:YAG laser. The laser beam is split by a 1-inch circular mirror which is cut into half[14] for the laser to strike both rods. Furthermore, a split vertical transverse stage allows for control of the laser fluence impinging on each beam separately. The clusters are cooled by addition of He carrier gas into the laser vaporization source.

Once formed, the clusters exit the source through a conical nozzle, and they enter the flow tube where oxygen reactant gas is added downstream at a reactant gas inlet. Most of the products and carrier gas are then pumped away by a high-volume roots pump, but those species that survive are sampled through a 1-mm orifice and focused by a set of electrostatic lenses into the quadrupole mass analyzer. The products are subsequently detected with a channel electron multiplier.

First-principles electronic structure investigations on Al_nAu^- clusters were carried out within a density functional formalism[15]. Here, the exchange correlation contributions were incorporated through a generalized gradient approximation (GGA) functional proposed by Perdew, Burke, and Ernzerhof[16]. The electronic orbitals and eigenstates were determined using a LCAO molecular orbital approach. Here, the wave function for the cluster is expressed as a linear combination of Gaussian-type orbitals centered at the atomic positions in the cluster. The actual calculations were carried out using the deMon2k software[17]. In this implementation, an auxiliary function set is used for the variational fitting of the Coulomb potential[18,19]. The numerical integration of the exchange-correlation energy and potential are performed on an adaptive grid[20].

For Au, we used the RECP19-electron pseudopotential from Stuttgart–Dresden[21] that includes scalar relativistic effects. For the effective core potential (ECP) integrals, a half-numeric integrator recently implemented in deMon2k [22] was used. In the present studies, we employed the double zeta

valence polarized (DZVP) basis sets[23] for Al and O and the RECP19 basis set for Au [21]. The GEN-A2 auxiliary function set for C and O and the GEN-A2* auxiliary function set for Au were used. The GEN-A2 auxiliary function set contains *s*, *p*, and *d* auxiliary functions and has been optimized for the DZVP basis set. The GEN-A2* auxiliary function set possesses a similar structure as the GEN-A2 set but includes also *f* and *g* functions. To determine the ground state, the configuration space was sampled by starting from several initial configurations and optimizing the geometry by moving atoms in the direction of forces. The geometries were optimized without any symmetry constraint using delocalized internal coordinates with the Broyden, Fletcher, Goldfarb, and Shanno (BFGS) update in the deMon2K program[24]. A structure optimization was converged if the root mean square of the gradient (RMSG) and the largest component of the delocalized internal gradient was smaller than 0.0003 and 0.0045 a.u., respectively. Additionally, either the root mean square of the delocalized internal displacement and the largest component of the displacement must be smaller than 0.0012 and 0.0018 a.u., respectively, or the change in energy between the previous two geometries must be smaller than 5×10^{-6} a.u. Since transition metal atoms are marked by non-zero spin multiplicities, the ground state determination included investigation over several spin multiplicities.

RESULTS AND DISCUSSION

The mass spectra for the Al_nAu_m clusters without reactant gas addition are shown in the top panel Fig. 1. As seen in these spectra, bimetallic clusters of Al_nAu_m with n = 3–24 and m = 0–2 are produced in varying compositions by ablating the two metal rods in our flow reactor system.

Upon the addition of increasing amounts of oxygen at a reactant gas inlet, certain species begin to arise from the mass spectrum as being stable, similar to the experiments reported previously in our laboratory for the stability of $Al_n^{+/-}$, $Al_nN_m^-$, $Al_nC_m^-$, and $Al_nX_m^-$ (X = halogen)[2–5,25–27]. From the spectra shown in Fig. 1, one can see that with the addition of increasing amounts of oxygen, most of the species begin to decrease in intensity and disappear from the distribution. However, there are species that are not "etched" by the oxygen and even increase in intensity with further oxygen addition. Looking at the spectrum which corresponds to the addition of 100 sccm (standard cubic centimeters per minute) of oxygen, it is shown that, in the middle panel of Fig. 1, the species that stand out after the oxygen addition are Al_{13}^-, Al_6Au^-, $Al_{10}Au^-$, $Al_{12}Au^-$, $Al_{14}Au^-$, and $Al_{16}Au^-$. However, Al_6Au^- is the only species in Fig. 1 that does not diminish in intensity

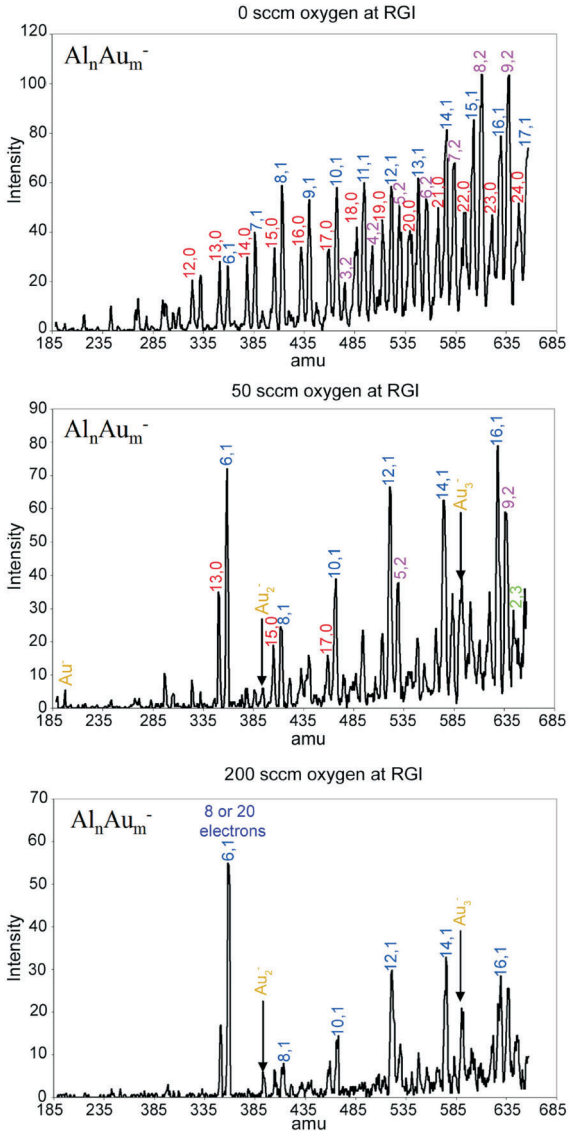

FIG. 1
Mass spectra of the unreacted and reacted $Al_nAu_m^-$ species

with the further addition of oxygen at the reactant gas inlet, as shown in the 200 sccm spectrum (bottom pane, Fig. 1). $Al_{10}Au^-$, $Al_{12}Au^-$, $Al_{14}Au^-$, and $Al_{16}Au^-$ are all shown to decrease in intensity between the spectrum where 50 sccm oxygen has been added and that with 200 sccm oxygen. As pointed out above, looking at Al_6Au^- in the context of the confined nearly free electron gas model, this cluster can correspond to either an 8 or 20 electron species, with Al contributing either one or three electrons, while Au donates a single electron.

In order to probe the stability of Al_6Au^-, we carried out theoretical studies on pure Al_n^- and Al_nAu^- clusters containing 4, 5, 6, and 7 Al atoms. The geometries and ground state spin multiplicities of pure Al_n^- clusters have been previously investigated, and our results agree with those investigations[11b,28]. For the clusters containing a Au atom, the Au atom was placed at the on-top, bridge, and hollow locations above the pure Al_n clusters. The geometry was optimized by moving atoms until the convergence criterion was reached. The calculations were repeated for various spin multiplicities to determine the ground state. As shown later, the oxygen etching can lead to the formation of neutral as well as ionic species. The investigations, therefore, covered both the anionic and neutral species. While the detailed results will be presented in a later publication, here we focus primarily on the stability of Al_6Au^-.

Figure 2 shows the ground state geometries of neutral aluminum, anionic aluminum, and anionic aluminum-gold clusters containing a single Au atom. Also shown are the spin multiplicities and the bond lengths (in Å). Note that, in all cases, the Au atoms occupy the hollow sites above the Al_n surface. Figure 2 also shows the highest occupied molecular orbital (HOMO) in Al_nAu^- clusters. Note that most of the contribution comes from the Al sites. In order to ascertain the accuracy of the theoretical studies, we calculated the vertical electron affinity of Al_6Au^- for which experimental values exist. Our calculated value of 2.78 eV is in excellent agreement with the measured value of 2.83 eV [29].

In order to examine the stability of clusters, we calculated the energy required to remove a single Al, a single Al^-, or a Au atom from the Al_nAu^- clusters. In Fig. 3a and 3b, we show the results of our investigations for pure Al_n^- and for Al_nAu^- clusters, respectively. Note that Al_n^- clusters show a maximum for the removal of an Al at $n = 6$, but they do not show any maxima at $n = 6$ for the removal of an Al^-. On the other hand, the Al_nAu^- clusters exhibit a maximum both for the removal of an Al atom and Al^- and also for the removal of an Au atom. While it takes 3.97 eV to remove an Al

atom from Al_6Au^-, it only takes 2.28 eV to remove an Al atom from Al_7Au^-. Similarly, while it takes 5.8 eV to remove an Al^- from Al_6Au^-, it only takes 4.6 eV to remove an Al^- from Al_7Au^-. Finally, while it takes 3.87 eV to remove a Au atom from Al_6Au^-, it only takes 3.06 eV to remove a Au atom from Al_7Au^-. This suggests that the observed growth of the Al_6Au^- upon exposure to oxygen, seen in the experiments where the clusters are exposed to oxygen (see Fig. 1), is most likely due to etching of the larger species. In order to more critically examine the etching of the clusters by oxygen, we considered the energetics of the following fragmentation channels.

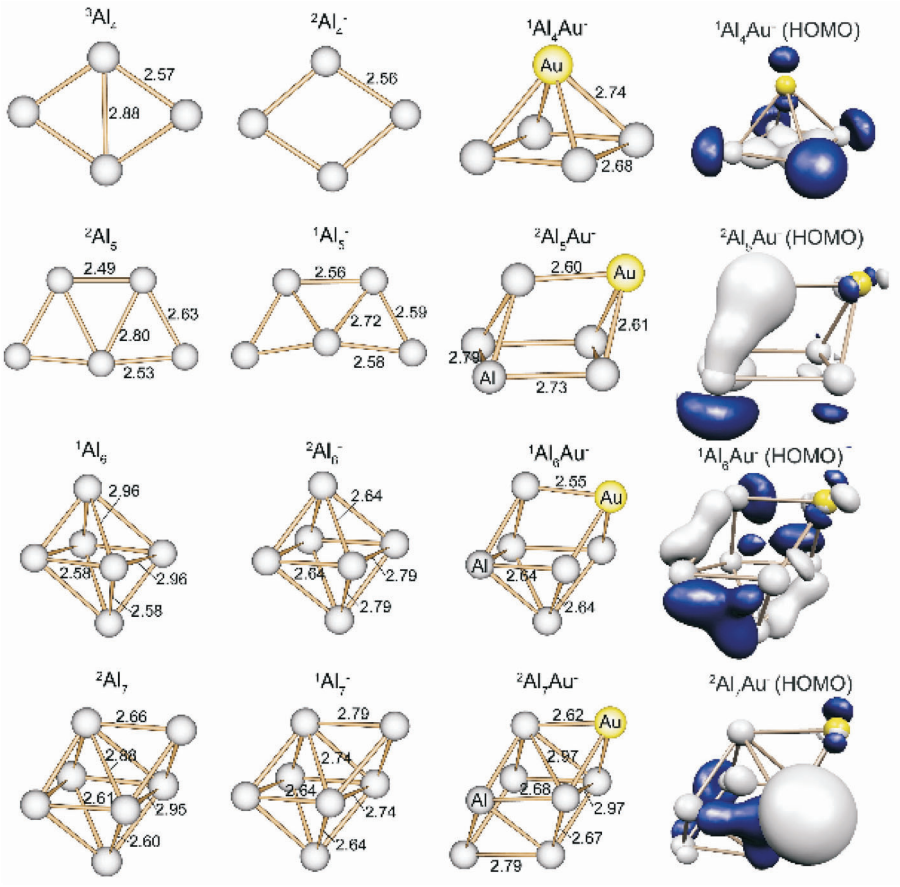

FIG. 2

Ground state geometries of Al_n, Al_n^-, and Al_nAu^- clusters. The bond lengths are in Å and superscripts indicate the spin multiplicity. Also shown is the electron charge density in the HOMO

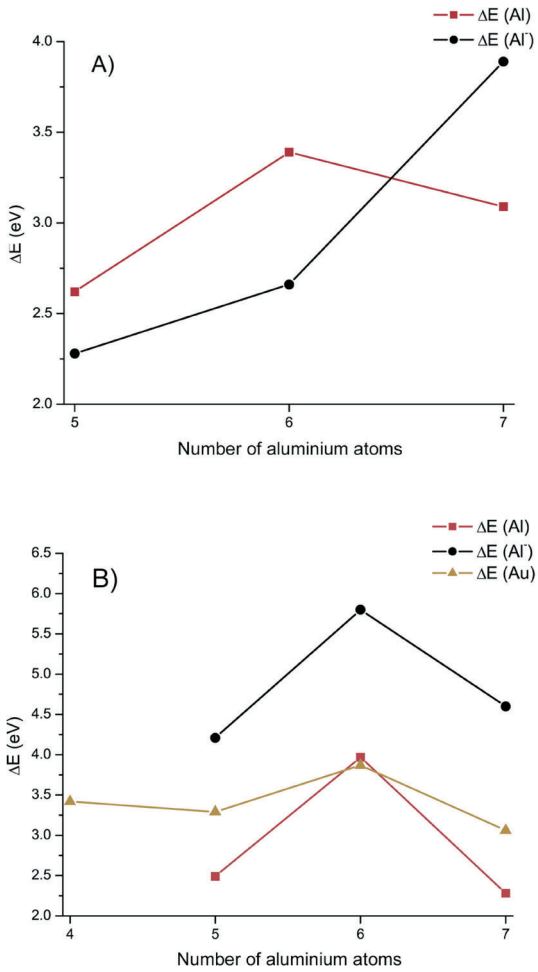

FIG. 3

A) The gain in energy in adding an Al (■) or an Al^- (●) to Al_n^- (n = 5–7) clusters. B) The gain in energy in adding an Al (■), and Al^- (●) or a Au (▲) to Al_nAu^- (n = 5–7) clusters

$$Al_nAu^- + O_2 \rightarrow Al_{n-1}Au^- + AlO_2 \quad (1)$$

$$Al_nAu^- + O_2 \rightarrow Al_{n-1}Au + AlO_2^- \quad (2)$$

$$Al_nAu^- + O_2 \rightarrow Al_{n-2}Au^- + Al_2O_2 \quad (3)$$

$$Al_nAu^- + O_2 \rightarrow Al_n^- + AuO_2 \quad (4)$$

$$Al_nAu^- + O_2 \rightarrow Al_n + AuO_2^- \quad (5)$$

For each of these channels, we compared the total energy of the reactants with the expected product. Note that, since the experiments are carried out under cold conditions, we only examined the reaction products where the O–O bond remains intact. For example, while the ground state of Al_2O_2 is a rhombus structure with no O–O bond, the formation of the ground state structure involves the breaking of the O–O bond. Our studies confirm that there is a barrier of 0.26 eV that can not be overcome under ordinary conditions. Similarly, while the ground state of AlO_2 is a triangular structure with no O–O bond, the formation of the ground state involves a barrier of 1.25 eV for the breaking of the O–O bond. Consequently, we only considered products with the O–O bond intact. Our calculated energies indicate that the reactions (*1*) and (*2*) are exothermic for Al_5Au^- with energies of 0.34 and 0.72, respectively. The same is true for Al_7Au^- where the corresponding energies for the reactions (*1*), (*2*), and (*3*) are 0.55, 0.33 and 0.50 eV, respectively. For Al_6Au^-, on the other hand, the reactions (*1*), (*2*), (*4*), and (*5*) are energetically prohibited by 1.14, 0.87, 3.39, and 3.59, respectively. However, the reaction (*3*) is exothermic by 0.29 eV. Since the ground state of Al_2O_2 has Al sites separated from each other by more than 3 Å while the Al–Al distance in Al_6Au^- is shorter, we investigated, in detail, such a process. An O_2 molecule was brought towards the Al_6Au^- cluster perpendicular to an Al–Al bond. The gain in energy was only 2.66 eV, while it takes 6.46 eV to remove 2 Al atoms, indicating that such a possibility is kinetically

prohibited. Hence, reaction (*3*) is not possible under conditions of the experiment, and Al_6Au^- appears as the magic species.

In order to further probe the mechanism underlying the stability of Al_6Au^-, we now consider the formation of Al_6Au^- by starting from the pure Al_6 and Au. To this end, we show in Fig. 4 the one-electron levels in Al_6, Al_6^-, the Au atom, and those in Al_6Au^-. The continuous lines correspond to the filled states, while the dotted lines correspond to unfilled levels. For the Au atom, we have included the filled 5d states in the valence manifold. The numbers beside the lines represent the degeneracy of the states. Note that the Au d- and s-states are within the manifold of the Al_6^- states and interact with the p-state of the Al sites, leading to a stable species with a

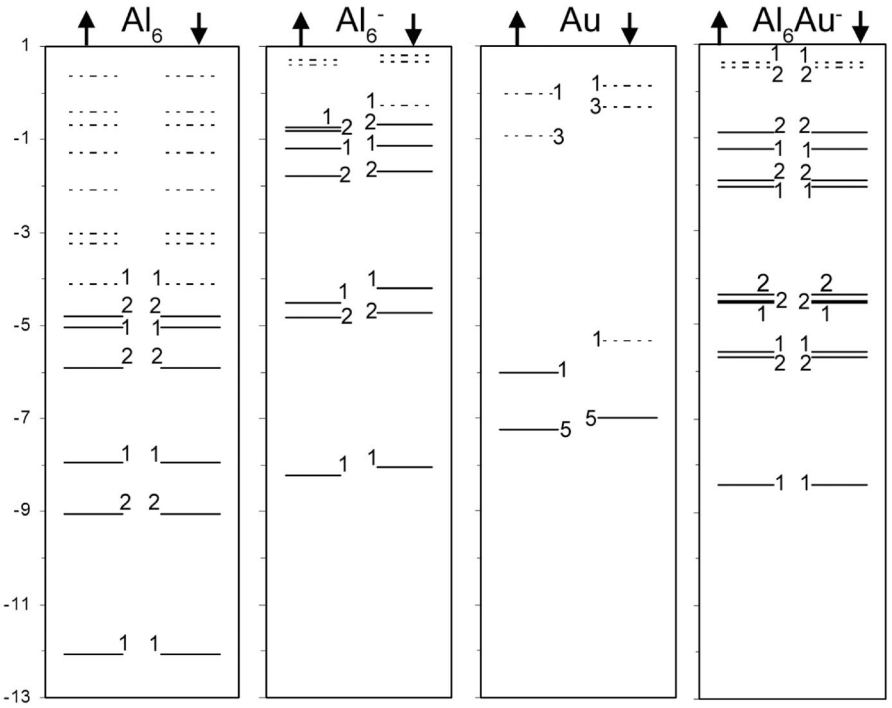

FIG. 4
The one-electron levels in Al_6, Al_6^-, Au, and Al_6Au^- clusters. The continuous lines correspond to the filled levels while the dotted lines correspond to unoccupied states. The degeneracies of the states are shown by numbers

HOMO-LUMO gap of 1.38 eV. The mixing between the states indicates that Al_6Au^- may be best described as a 20-electron system (assuming that the d-states of Au are localized around the Au atom and are not counted in the nearly free electron gas). We would like to add that the definition of a jellium density and shape for a compound cluster is not trivial. Consequently, a more quantitative comparison with the jellium picture is difficult.

CONCLUSIONS

To summarize, the synergistic studies employing experiments and first principles electronic structure calculations are used to show that Al_6Au^- is an unusually stable species marked by a large HOMO-LUMO gap and increased energy to remove an Al and Au atom. There is substantial mixing between the Au d- and s-states and the sp-states of the Al_6^-, and the system is best described as a nearly free electron gas with a shell closing of 20 electrons. We are currently extending our studies to other systems, and these results will be reported in a subsequent publication.

A. W. Castleman and M. L. Kimble gratefully acknowledge support from U.S. Air Force Office of Scientific Research grant F49620-01-1-0328 while J. U. Reveles and S. N. Khanna acknowledge support from U.S. Air Force Office of Scientific Research grant FA9550-05-1-0186 for the theoretical work on these systems. The authors are equally grateful to U.S. Department of the Army for support through a MURI grant No. W911NF-06-1-0280. S. N. Khanna is also grateful to VCU for providing a study/research leave. The authors thank P. J. Roach for valuable discussions and assistance in the work.

REFERENCES

1. Sanchez A., Abbet S., Heiz U., Schneider W. D., Häkkinen H., Barnett R. N., Landman U.: *J. Phys. Chem. A* **1999**, *103*, 9573.
2. Leuchtner R. E., Harms A. C., Castleman A. W., Jr.: *J. Chem. Phys.* **1989**, *91*, 2753.
3. Bergeron D. E., Castleman A. W., Jr., Morisato T., Khanna S. N.: *Science* **2004**, *304*, 84.
4. Bergeron D. E., Roach P. J., Castleman A. W., Jr., Jones N. O., Khanna S. N.: *Science* **2005**, *307*, 231.
5. Bergeron D. E., Roach P. J., Castleman A. W., Jr., Jones N. O., Reveles J. U., Khanna S. N.: *J. Am. Chem. Soc.* **2005**, *127*, 16048.
6. Knight W. D., Clemenger K., de Heer W. A., Saunders W. A., Chou M. Y., Cohen M. L.: *Phys. Rev. Lett.* **1984**, *52*, 2141.
7. de Heer W. A., Knight W. D., Chou M. Y., Cohen M. L.: *Solid State Phys.* **1987**, *40*, 93.
8. Reveles J. U., Khanna S. N., Roach P. J., Castleman A. W., Jr.: *Proc. Natl. Acad. Sci.* **2006**, *103*, 18405.
9. Khanna S. N., Jena P.: *Phys. Rev. Lett.* **1992**, *69*, 1664.

10. Pederson M. R. in: *Physics and Chemistry of Finite Systems: From Clusters to Crystals* (P. Jena, S. N. Khanna and B. K. Rao, Eds), Vol. II, pp. 861–866. Kluwer, Dordrecht 1992.
11. a) Li X., Wu H., Wang X.-B., Wang L.-S.: *Phys. Rev. Lett.* **1998**, *81*, 1909; b) Rao B. K., Jena P.: *J. Chem. Phys.* **1999**, *111*, 1890.
12. Castleman A. W., Jr., Weil K. G., Sigsworth R. E., Leuchtner R. E., Keesee R. G.: *J. Chem. Phys.* **1987**, *86*, 3829.
13. Leuchtner R. E., Harms A. C., Castleman A. W., Jr.: *J. Chem. Phys.* **1990**, *92*, 6527.
14. Wagner R. L., Vann W. D., Castleman A. W., Jr.: *Rev. Sci. Instrum.* **1997**, *68*, 3010.
15. Kohn W., Sham L. S.: *Phys. Rev. At., Mol., Opt. Phys.* **1965**, *140*, 1133.
16. Perdew J. P., Burke K., Ernzerhof M.: *Phys. Rev. Lett.* **1996**, *77*, 3865.
17. Köster A. M., Calaminici P., Casida M. E., Flores-Moreno R., Geudtner G., Goursot A., Heine T., Ipatov A., Janetzko F., del Campo J. M., Patchovskii S., Reveles J. U., Salahub D. R., Vela A.: *deMon2k*, V. 2.3. deMon Developers 2006.
18. Dunlap B. I., Connolly J. W. D., Sabin J. R.: *J. Chem. Phys.* **1979**, *71*, 4993.
19. Mintmire J. W., Dunlap B. I.: *Phys. Rev. A* **1982**, *25*, 88.
20. Köster A. M., Flores-Moreno R., Reveles J. U.: *J. Chem. Phys.* **2004**, *121*, 681.
21. Schwerdtfeger P., Dolg M., Schwarz W. H. E., Bowmaker G. A., Boyd P. D. W.: *J. Chem. Phys.* **1989**, *91*, 1762.
22. Flores-Moreno R., Alvarez-Mendez R. J., Vela A., Köster A. M.: *J. Comput. Chem.* **2006**, *27*, 1009.
23. Godbout N., Salahub D. R., Andzelm J., Wimmer E.: *Can. J. Chem.* **1992**, *70*, 560.
24. Reveles J. U., Köster A. M.: *J. Comput. Chem.* **2004**, *25*, 1109.
25. Leuchtner R. E., Harms A. C., Castleman A. W., Jr.: *J. Chem. Phys.* **1991**, *94*, 1093.
26. Leskiw B. D., Castleman A. W., Jr., Ashman C., Khanna S. N.: *J. Chem. Phys.* **2001**, *114*, 1165.
27. Leskiw B. D., Castleman A. W., Jr.: *Chem. Phys. Lett.* **2000**, *316*, 31.
28. Sun J., Lu W. C., Wang H., Li Z.-S., Sun C.-C.: *J. Phys. Chem. A* **2006**, *110*, 2729.
29. Kuznetsov A. E., Boldyrev A. I., Zhai H.-J., Wang L.-S.: *J. Am. Chem. Soc.* **2002**, *124*, 11791.